

Journal Pre-proof

Effects of burn severity on organic nitrogen and carbon chemistry in high-elevation forest soils

Holly K. Roth, Amy M. McKenna, Myrna J. Simpson, Huan Chen, Nivetha Srikanthan, Timothy S. Fegel, Amelia R. Nelson, Charles C. Rhoades, Michael J. Wilkins, Thomas Borch

PII: S2949-9194(23)00023-7

DOI: <https://doi.org/10.1016/j.seh.2023.100023>

Reference: SEH 100023

To appear in: *Soil & Environmental Health*

Received Date: 7 February 2023

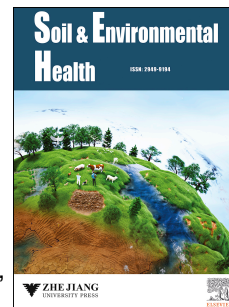
Revised Date: 14 June 2023

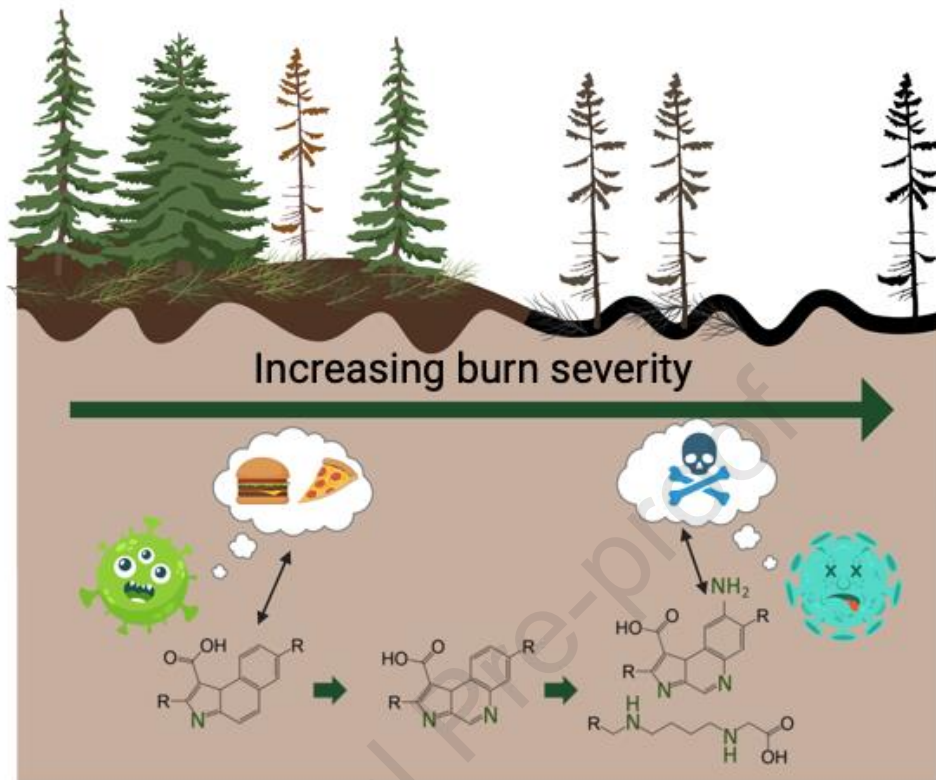
Accepted Date: 14 June 2023

Please cite this article as: Roth, H.K., McKenna, A.M., Simpson, M.J., Chen, H., Srikanthan, N., Fegel, T.S., Nelson, A.R., Rhoades, C.C., Wilkins, M.J., Borch, T., Effects of burn severity on organic nitrogen and carbon chemistry in high-elevation forest soils, *Soil & Environmental Health*, <https://doi.org/10.1016/j.seh.2023.100023>.

This is a PDF file of an article that has undergone enhancements after acceptance, such as the addition of a cover page and metadata, and formatting for readability, but it is not yet the definitive version of record. This version will undergo additional copyediting, typesetting and review before it is published in its final form, but we are providing this version to give early visibility of the article. Please note that, during the production process, errors may be discovered which could affect the content, and all legal disclaimers that apply to the journal pertain.

© 2023 The Author(s). Published by Elsevier B.V. on behalf of Zhejiang University and Zhejiang University Press Co., Ltd.





Effects of burn severity on organic nitrogen and carbon chemistry in high-elevation forest soils

Holly K. Roth¹, Amy M. McKenna^{2,3}, Myrna J. Simpson⁴, Huan Chen², Nivetha Srikanthan⁴, Timothy S. Fegel⁵, Amelia R. Nelson³, Charles C. Rhoades⁵, Michael J. Wilkins³, Thomas Borch^{1,3*}

¹Department of Chemistry, Colorado State University, Fort Collins, CO, USA, 80523

²National High Magnetic Field Laboratory, Ion Cyclotron Resonance Facility, Florida State University, FL, USA

³Department of Soil and Crop Sciences, Colorado State University, Fort Collins, CO, USA , 80523

⁴Environmental NMR Centre and Department of Physical & Environmental Sciences, University of Toronto Scarborough, Toronto, Ontario, Canada

⁵Rocky Mountain Research Station, U.S. Forest Service, Fort Collins, CO, USA

* Corresponding author

Abstract

Fire frequency and severity have increased in recent decades in the western United States, which have direct implications for the quantity and composition of soil organic matter (SOM). While the effects of wildfire on soil carbon (C) and inorganic nitrogen (N) have been well studied, little is known about the impacts of fire on soil organic N. Since organic N is the most abundant form of soil N in conifer forests and dominant source of plant N facilitated by symbiotic mycorrhizae and mineralization, better understanding of post-fire organic N chemistry will help address a critical gap in our understanding of fire effects on SOM. Here, we characterized changes to organic N chemistry across fire severity gradients resulting from two wildfires that burned lodgepole pine (*Pinus contorta*) forest along the Colorado/Wyoming border, USA. One representative gradient was selected for high-resolution analysis based on results from bulk data (total C and N, pH). Mineral soils were collected from two depths in low, moderate, and high severity burned areas and adjacent, unburned locations one year following the Ryan and Badger Creek fires. Nuclear magnetic resonance spectroscopy and ultrahigh-resolution Fourier transform ion cyclotron resonance mass spectrometry analysis showed that N content and aromaticity of water-extractable SOM (0-5 cm depth) increased with burn severity, while minimal changes to 5-10 cm depth were observed. Heterocyclic N species are generally higher in toxicity compared to their non-nitrogenated counterparts, which prompted soil toxicity measurements. Complementary Microtox® analysis revealed a positive relationship between increased fire severity and increased soil toxicity to *Aliivibrio fischeri* (microbial test species). These findings add to our molecular-level understanding of organic C and N responses to wildfire severity, with likely implications for nutrient cycling, forest recovery and water quality following severe wildfire.

Keywords: burn severity, soil organic matter, organic nitrogen, FT-ICR MS, toxicity, NMR spectroscopy

45 1 Introduction

46 Wildfire activity in the western United States has increased in recent decades in terms of the
47 size of area burned (Williams and Abatzoglou, 2016) and the frequency and severity of large fires
48 (Abatzoglou et al., 2017), and is projected to continue to increase (Westerling, 2016). Observed
49 warming conditions have led to greater frequency of wildfire in high-elevation forest in recent
50 years (Alizadeh et al., 2021); therefore, it is critical that we understand the impacts of changing
51 fire regimes on ecosystem dynamics, biodiversity, and productivity at higher elevations. The
52 expected increase in burn severity (i.e., degree of consumption of organic soil layers and
53 vegetation) (Parsons et al., 2010) may have implications for carbon cycling, potentially shifting
54 forests from C sinks to C sources. The post-fire soil organic matter (SOM) composition provides
55 a baseline for a forest's recovery; thus, molecular-level analysis of SOM from different burn
56 severities will help improve our understanding of ecosystem response following wildfire.

57 Wildfires influence biogeochemical and hydrological cycles through the combustion of
58 biomass, which alters SOM properties (e.g., C:N:P stoichiometry, pH, major functional groups),
59 forms hydrophobic layers, and increases C and N in postfire runoff (González-Pérez et al., 2004).
60 The combination of heat from wildfires and changes in SOM properties have consequences for
61 plant and microbiome diversity which may persist for years after the fire. Previous studies indicate
62 that burn severity differentially impacts the upper 5 cm of mineral soil (Hartford and Frandsen,
63 1992) and local soil microbiomes by destabilizing soil aggregates and affecting microbial biomass
64 and composition and associated enzyme activity (Pulido-Chavez et al., 2021). SOM
65 transformations that occur during heating can result in increased chemical heterogeneity, forming
66 a substrate that is generally more resistant to microbial decomposition (Singh et al., 2012). SOM
67 and soil microbiota are important for re-establishment of native plant species; therefore, fire-
68 induced transformations may influence post-fire plant succession, plant species composition, and
69 ecosystem processes (Turner, 2010). Short-term (1-5 years post-fire) impacts often include
70 significant SOM losses from surface organic horizons (Nave et al., 2011). Additional short-term
71 responses include increased erosion (Moody et al., 2013), increased inorganic N (Wan et al., 2001),
72 and decreased bacterial and fungal community richness in burned plots compared to unburned
73 (Caiafa et al., 2023; Nelson et al., 2022; Pulido-Chavez et al., 2021). Negative impacts to soil
74 microbes may persist for over a decade; ectomycorrhizal and saprobic richness were lower than in
75 unburned soils 11 years after fire in a ponderosa pine (*Pinus ponderosa*) forest (Pulido-Chavez et
76 al., 2021), total soil N depletion persisted at least 14 years following fire with subsequent reduction
77 of tree and shrub colonization in a Scots pine (*P. sylvestris*) forest (Dzwonko et al., 2015), and
78 dissolved total nitrogen (DTN) export was ~10x higher in burned compared to unburned
79 catchments 14 years after the Hayman Fire in Colorado (Rhoades et al., 2018). Recovery of
80 microbial communities requires bioavailable C and N, therefore, understanding the role of burn
81 severity on SOM C and N composition is important for developing effective post-fire management
82 strategies.

83 Organic N is a dynamic component of soils, derived primarily from amino acids and peptides
84 and easily mineralized into plant-available inorganic N (Zhong and Makeshin, 2003). Organic N
85 comprises 62-83% of the total N in Norway spruce stands (Smolander et al., 2001), and dissolved
86 organic N (DON) is a primary pathway for N loss in forest soils while acting as a N source for
87 mycorrhizal plants in boreal forests (Andersson et al., 2000). Direct analysis of organic N can be
88 accomplished by Fourier transform ion cyclotron resonance mass spectrometry (FT-ICR MS),
89 which provides molecular-level insight that can be used to calculate oxidation state, aromaticity,
90 and biolability (D'Andrilli et al., 2015). Acidic N species in burned SOM detected by negative-

91 ion electrospray ionization (-ESI) FT-ICR MS indicate that N incorporates into refractory,
92 heterocyclic aromatic compounds that are more resistant to microbial degradation (Luo et al.,
93 2019; Roth et al., 2022b). Bahureksa and coworkers reported that aromatic N heterocycles were
94 formed in soil burned at higher temperatures in a laboratory microcosm (Bahureksa et al., 2022);
95 however, these findings have not yet been verified across burn severities. Additionally, positive-
96 ion mode ESI detected more than twice the number of N-species across a wider H/C and O/C range
97 compared to -ESI in fire-affected soils (Roth et al., 2022a). Thus, in this study we focus on +ESI
98 to selectively ionize SOM species through protonation reactions to catalogue molecular
99 transformations that occur during soil heating and the potential implications for N cycling.

100 Nuclear magnetic resonance (NMR) spectroscopy can be paired with FT-ICR MS to quantify
101 shifts in functionality, which is required to link SOM compositional changes to microbial
102 degradation pathways to improve C and N cycling predictions in response to high severity fires
103 (Schmidt et al., 2011). NMR has been used to demonstrate an increase in aromatic structures and
104 decrease in alkylated organic molecules in severely burned pine forest soils (Knicker et al., 2008).
105 NMR spectra showing decreased atomic H/C and O/C ratios across a burn severity gradient in
106 soils from wildfire-affected forest and shrub ecosystems are the net result of greater dehydration,
107 dealkylation, and decarboxylation reactions at higher wildfire severity (Merino et al., 2015). The
108 abundance of N-heterocyclic compounds also increased with burn severity, but varied with fuel
109 composition (e.g., grasses or coniferous litter) and heating conditions (Bahureksa et al., 2022;
110 Merino et al., 2015; Roth et al., 2022a). However, rigorous analysis of the specific compounds
111 formed at different burn severities remains limited, especially in field studies.

112 Wildfires have been reported to release toxic compounds (e.g., polycyclic aromatic
113 hydrocarbons; PAHs, heavy metals, nitrogenated species), with associated short- and long-term
114 implications for ecosystem recovery due to their environmental persistence and propensity to
115 bioaccumulate. Importantly, N-heterocycles have been linked to increased toxicity in
116 hydrothermal liquefaction of biomass (Alimoradi et al., 2020) and have been shown to modulate
117 the toxicity of co-occurring metals in soils (i.e., cadmium, boron) (Cervilla et al., 2009), although
118 specific structures have yet to be reported. Ecotoxicants may prompt shifts in microbial
119 populations that adversely affect ecosystem processes or may be transported downslope in leachate
120 or eroding soil or downstream in surface runoff. Microtox® is a bioassay that uses
121 bioluminescence inhibition of the bacterium *Aliivibrio fischeri* (*A. fischeri*) to evaluate chemical
122 contamination in soils, waters, and biochars, (Gavrić et al., 2022) and is commonly used as an
123 indicator for metal, pesticide, or PAH contamination (Doherty, 2001). Limited studies exist on the
124 eco-toxicological impacts of fire on water quality, despite evidence that post-fire runoff is toxic to
125 organisms in multiple trophic groups (Campos et al., 2012). Therefore, the impact of burn severity
126 on soil toxicity is relatively unexplored.

127 Here, we characterize the relationship between fire severity and SOM composition along
128 soil burn severity gradients and discuss the implications of N-heterocycle formation for toxicity to
129 soil microbes. Soil was collected from two recently burned lodgepole pine dominated forests along
130 the Colorado-Wyoming border (**Figure 1**). We hypothesized that soil C and N chemical
131 composition would track with burn severity with more microbially-recalcitrant organic matter and
132 heterocyclic N compounds formed at higher burn severities. To evaluate this hypothesis, we
133 measured elemental chemistry across four distinct burn severity gradients at wildfires near the
134 Colorado-Wyoming border and then performed a suite of high-resolution analyses which included
135 NMR, FT-ICR MS and Microtox® on one representative burn severity gradient. We found that
136 molecular-level C and N composition differed with burn severity. The chemical patterns we

137 identified may have relevance to soil toxicity to microbes, though verification of its general
138 importance requires exploration across wide temporal and ecosystem ranges.

139

140 2 Methods

141 2.1 Soil Sampling and Preparation

142 Soil samples were collected in mid-2019, one-year post-fire in lodgepole pine-dominated
143 forests burned by the 2018 Badger Creek and Ryan fires in the Medicine Bow National Forest
144 (elevation 2500-2750 m). The sampling period captures the conditions the first summer following
145 fire and snowmelt, when the site was first accessible. Soils in the sampling areas were loamy-
146 skeletal Ustic Haplocrypts and fine-loamy Ustic Haplocryalfs.

147 Four independent burn severity gradients comprised of low, moderate, and high severity
148 burns and an unburned control were selected based on remotely sensed comparison of pre- and
149 post-fire greenness (Key and Benson, 2006). Severity was field-validated prior to sampling using
150 standard soil burn severity indicators (Parsons et al., 2010). Low, moderate, and high severity sites
151 had >85%, 20-85%, and <20% O-horizon cover, respectively (Parsons et al., 2010). At each
152 sampling site, a 3x5 m sampling grid with 6 m² subplots was laid out perpendicular to the dominant
153 slope (**Figure 1**). To limit differences in site aspect, slope gradient, and pre-fire vegetation within
154 each of the burn severity gradients, we located individual burn severity classes within 50 m of one
155 another.

156 A sterilized trowel was used to collect approximately 150 g of 0-5 cm and 5-10 cm soils
157 by first sampling and collecting the 0-5 cm soil, then collecting the underlying 5-10 cm soil.
158 Samples (n = 48) were placed on ice in the field and stored at 4°C in the laboratory until processing.
159 The unburned control and low severity samples had a thin O-horizon (~5 mm), and the moderate
160 and high severity samples had a similar thickness of charred organic matter and ash. After air
161 drying, samples were passed through a 2-mm mesh sieve to remove residual litter and other large
162 debris. See Nelson et al. for additional details (Nelson et al., 2022).

163
164 **Elemental Measurements** Dissolved organic carbon (DOC) and dissolved total nitrogen (DTN)
165 concentrations were determined from warm water extracts (1:2, soil:water) for the soil samples.
166 Measurements were performed with a TOC-VCPN total organic C/N analyzer (Shimadzu
167 Corporation, Columbia, MD, USA). A subset of samples from each depth (n = 16) were dried (48
168 h at 60°C), ground to a fine powder, and analyzed for total C and N by dry combustion (LECO
169 Corporation, St. Joseph, MI, USA). To determine the pH of the soils, a 1:2 ratio of soil (g) to
170 deionized water (mL) was shaken for 1 hour at 200 rpm before pH measurements were recorded.
171 We used the DOC and DTN concentrations and pH (Table S1) to identify general patterns and
172 select a subset of representative samples (n = 6; n = 4 for 0-5 cm and n = 2 for 5-10 cm) for selected
173 analyses.

174
175 **Soil extractions:** We identified significant differences in DOC and DTN concentrations between
176 the 0-5 cm unburned control and moderate and high severity water extracts, as well as a significant
177 difference in pH between the control and all burned 0-5 cm soil water extracts (**Table S1**). We
178 also noted significant differences in %C and %N between the unburned control and moderate and
179 high 0-5 cm soils (**Table S2**). Based on these differences in soils between each burn severity class
180 at the 0-5 cm depth, a single gradient consisting of one control and one each of the low, moderate,
181 and high severity soils (n = 1 for four total samples) were selected for further analysis described
182 below. Since there were no differences in the 5-10 cm soils or water extracts; two samples were

183 selected for further analysis from the deep samples (control and moderate) as differences in soil
184 chemistry were expected to be minimal. A total of six samples from the 48 collected were selected
185 for further analyses, including acute toxicity, 21 tesla FT-ICR MS, and solid-state ^{13}C NMR: a
186 high severity 0-5 cm soil, moderate severity 0-5 cm and 5-10 cm soils, a low severity 0-5 cm soil,
187 and controls from the 0-5 cm and 5-10 cm soils (**Table S3**).

188 Dissolved organic matter (DOM) using water extracts of the 0-5 cm soils from this subset
189 was also analyzed by solution-state ^1H NMR. For acute toxicity and FT-ICR MS, 50 g dry, sieved
190 soil was weighed into a polystyrene weigh boat and transferred to a 250 mL Erlenmeyer flask. For
191 solution-state ^1H NMR, we used the DOC concentrations to determine the amount of soil needed
192 to extract 10 mg of DOC. For all samples, Millipore water was added to a final ratio of 1 g soil : 2
193 mL water in Erlenmeyer flasks (one flask for FT-ICR MS and acute toxicity, another for ^1H NMR),
194 which were covered with parafilm and shaken (10 hours, 170 rpm) in the dark. Water and soil
195 slurries were quantitatively transferred to pre-rinsed 50-mL centrifuge tubes with an additional
196 150 mL Millipore water. The samples were then centrifuged at 7500 rpm (756 x g) for 10 minutes,
197 during which a vacuum filtration system was assembled using acid-washed, pre-combusted
198 glassware. The 0.2 μm polyethersulfone (PES) filters were pre-rinsed with 100-150 mL Millipore
199 water prior to sample introduction. A 50-mL aliquot from the FT-ICR MS samples was stored in
200 centrifuge tubes; the remaining filtrate was stored in amber bottles at 4°C until solid phase
201 extractions. Solid soils were analyzed by solid-state ^{13}C NMR, and soil water extracts were
202 analyzed by solution-state ^1H NMR, 21 tesla FT-ICR MS, and Microtox®. Additional information
203 on NMR instrumentation can be found in Supporting Information.

204
205 **Acute toxicity of water-soluble species:** Microtox® acute toxicity analysis was used to determine
206 the toxicity of soil water extracts in the control and burned samples for *A. fischeri* bacteria. During
207 sample preparation for FT-ICR MS, 50 mL of each sample was subsampled and stored in
208 centrifuge tubes. From these samples, 1 mL was transferred to amber HPLC vials (3 mL for
209 RYN_126 only) for Microtox® analysis. Samples were carbon normalized to 9.29 ppm of C based
210 on DOC values and stored at 4°C until analysis. The percent decrease in bioluminescence of *A.*
211 *fischeri* bacteria after a 15-minute incubation period determines the toxicity of each sample based
212 on the amount of light emitted by the bacteria (Adams et al., 2015). The Microtox® 81.9%
213 screening test protocol was used on the Microtox® model 500 analyzer (Modern Water, New
214 Castle, DE, USA) as previously described (Chen et al., 2022b).

215
216 **2.2 FT-ICR MS Analyses**
217 **Solid-phase extractions:** Solid-phase extractions were performed on the six subsamples selected
218 for compositional analysis prior to FT-ICR MS analysis according to Dittmar et al. (Dittmar et al.,
219 2008). Briefly, samples were brought to room temperature and acidified to pH 2 with trace-metal
220 free hydrochloric acid (Sigma-Aldrich Chemical, St. Louis, MO, USA). PPL cartridges (Bond Elut
221 PPL (Priority PollutantTM), a styrene-divinylbenzene (SDVB) polymer modified with a proprietary
222 nonpolar surface) were rinsed with 15 mL HPLC-grade methanol (Sigma-Aldrich Chemical) and
223 15 mL of pH 2 Millipore water. Polar species in the water samples were retained on the sorbent,
224 rinsed with 15 mL of pH 2 water to remove salts, and allowed to dry overnight. Each sample was
225 recovered from the cartridge by elution with 2 mL HPLC-grade methanol and transferred to 2-mL
226 borosilicate vials prior to 21 tesla FT-ICR MS analysis.

227

228 **ESI Source:** All solvents were HPLC grade (Sigma-Aldrich Chemical) and SPE extracts were
229 analyzed after further dilution in methanol (1:10, by volume) prior to analysis by negative and
230 positive ion electrospray ionization. Sample solution was infused via a microelectrospray source
231 (Emmett et al., 1998) (50 μm i.d. fused silica emitter) at 500 nL/min by a syringe pump. Typical
232 conditions for negative ion formation were: emitter voltage, -2.7-3.1 kV; S-lens RF: (45 %) and
233 heated metal capillary temperature 350 °C. Positive-ion ESI spray conditions were opposite in
234 polarity.

235
236 **21 T FT-ICR MS:** The six DOM extracts were analyzed with a custom-built hybrid linear
237 ion trap FT-ICR mass spectrometer equipped with a 21 T superconducting solenoid magnet
238 (Hendrickson et al., 2015; Smith et al., 2018) and automatic gain control (AGC ion target:
239 1E6) (Belov et al., 2003; Page et al., 2005). Peaks with signal magnitude greater than 6
240 times the baseline root-mean-square (rms) noise at m/z 500 were exported to peak lists, and
241 molecular formula assignments and data visualization were performed with PetroOrg©
242 software (Corilo, 2014). Molecular formula assignments with an error >0.2 parts-per-
243 million were discarded, and only chemical classes with a combined relative abundance of
244 $\geq 0.10\%$ of the total were considered. All FT-ICR mass spectra files and assigned elemental
245 compositions are publicly available via the Open Science Framework at
246 <https://osf.io/758ux/> (DOI: DOI 10.17605/OSF.IO/758UX). Further details can be found
247 in Supporting Information.

248
249 2.3 MAG annotation for N heterocycle degradation genes

250 To investigate whether the soil microbiome was expressing genes for degrading N
251 heterocycles, we utilized the metagenome-assembled genome (MAG) and metatranscriptomic
252 dataset presented in Nelson et al. (2022) (NCBI BioProject PRJNA682830). We analyzed a MAG
253 dataset which was assembled from metagenomic sequencing done on 12 samples that consisted of
254 a triplicate of high severity and low severity (3 from 0-5 cm and 3 from 5-10 cm for each
255 treatment). We used HMMER (Eddy, 2011) against hidden Markov models (HMMs) curated from
256 UniProt (Bateman et al., 2015) to search for the genes needed to constitute the multicomponent
257 enzyme carbazole 1,9a-dioxygenase (CARDO) (Nojiri et al., 2005; Xu et al., 2006). CARDO is
258 made up of four parts: two terminal oxygenases (*carAa*; PF11723), a ferredoxin (*carAc*; PF00355),
259 and a ferredoxin reductase (*carAd*; PF00970, PF00111, PF00175). Following the identification of
260 the genes, we used the metatranscriptomics mapping data presented in Nelson et al. (2022) (Nelson
261 et al., 2022) to identify whether the genes were being expressed within the given MAG.

262
263 3 Results and Discussions

264
265 3.1 Burned soil organic matter is more complex than unburned

266 We performed solid-state ^{13}C NMR spectroscopy on six mineral soil samples to visualize
267 the differences in organic matter functionality across the burn severity gradient, with spectra
268 reported in **Figure S1** and integration results in **Table 1**. We chose to analyze the ^{13}C isotope due
269 to the low abundance of ^{15}N in natural samples. In the 0-5 cm soils, there was a decrease in alkyl
270 C and *O*-alkyl C from the unburned control to the low severity soil, consistent with the results
271 reported for *Pinus pinaster* duff, which indicated a dominance of alkyl C and *O*-alkyl C compounds
272 in the unburned sample (Merino et al., 2018). Conversely, aromatic and phenolic C was
273 approximately 3x higher in the low severity soil, indicative of incomplete combustion (Bodí et al.,

274 2014). The alkyl/*O*-alkyl C ratio, used as an indicator of SOM decomposition (a higher ratio
275 indicates a higher relative stage of decomposition) (Simpson et al., 2008), nearly doubled in the
276 low severity soil compared to the control. From low to moderate severity, the relative proportion
277 of alkyl C and *O*-alkyl C increased in the moderate severity 0-5 cm soil, then decreased slightly
278 from moderate to high. These shifts primarily resulted in decreases in the relative proportion of
279 aromatic and phenolic C in the moderate and high severity samples; carboxylic + carbonyl C were
280 slightly higher in the moderate and high severity 0-5 cm soils compared to the control. Importantly,
281 the alkyl/*O*-alkyl C ratio remained approximately double that of the control in all burned samples,
282 which indicates that fire drives SOM chemistry towards more complex forms that are less preferred
283 microbial substrates in this burn severity gradient. This is also reflected in the aromatic C
284 integration data (higher in burned soils), as aromatic C is generally considered to be less labile for
285 microbial respiration than other C forms (Schmidt and Noack, 2000). However, a separate study
286 on the same samples presented here found that microbial genes targeting aromatic compounds
287 were present in the soils (Nelson et al., 2022), which indicates that aromatic substrates can be
288 utilized as C sources in the burned soils.

289

290 3.2 DOM displays burn severity-dependent trends in 0-5 cm soils

291 We collected FT-ICR mass spectra for six soil water extracts along the burn severity
292 gradient – four from 0-5 cm soils (CNTL-S, LS-S, MS-S, HS-S) and two from 5-10 cm soils
293 (CNTL-NS, MS-NS). To increase compositional coverage, we ionized samples in ESI negative
294 and positive modes (Roth et al., 2022a). There were an average of 11320 assigned species in -ESI
295 and 21377 in +ESI, and a substantial increase in the number of nitrogenated species in the burned
296 soils relative to the unburned control, consistent with previously reported increases of CHNO in
297 fire-impacted water extracts of Jeffrey pine (*P. jeffreyi*) needles and woody trunks in -ESI (Chen
298 et al., 2022a). We plotted all elemental compositions identified in the analysis of the water-soluble
299 soil extracts in van Krevelen diagrams (H/C vs O/C) (Kim et al., 2003) to provide visualization of
300 the data and highlight compositional differences between the samples in **Figure 2**. Fire-impacted
301 samples spanned a wide range of H/C ratios (0.2-1.9), with a larger relative abundance of highly
302 saturated compounds in the low and high severity burn samples. Maximum O/C ratios decreased
303 with burn severity, as did average O/C (**Table S4**), consistent with carbonization and aromatization
304 processes and a decrease in the lability of soil species reported for *P. pinaster* soils (Merino et al.,
305 2018). Within the N-containing species, we again observed an enrichment in highly saturated
306 compounds in the low and high severity soils. O/C ratios in the nitrogenated species did not appear
307 to be as dependent on burn severity as the total assignments, which demonstrates that the O/C ratio
308 is likely not a primary driver for biotic or abiotic transformations of these species.

309

310 To further analyze the difference in DOM chemistry between burn severity classes, we also
311 performed solution-state ¹H NMR spectroscopy on DOM isolated from 0-5 cm soils in the burn
312 severity gradient (**Table 2**). Relative to the control, there was little to no change in the relative
313 proportion of materials derived from linear terpenoids (MDLT). Carboxyl-rich alicyclic molecules
314 (CRAM) were lower in the burned samples, consistent with lower average O and O/C and lower
315 average molecular weight in the FT-ICR mass spectra. Conversely, the relative contribution of
316 soluble carbohydrates and peptides was higher in the burned samples, with a maximum intensity
317 in the low severity soil extract, possibly indicative of cell lysis and residual necromass left behind
318 after fire (Donhauser et al., 2021), and compounded by the lightly combusted organic layer in the
319 low severity soil. The relative contribution of aromatic and phenolic functional groups reached a

320 maximum in the moderate severity soil extract, consistent with the calculated DBE and aromaticity
321 index in the FT-ICR mass spectra (**Table S5**). These results are generally supported by previous
322 studies across a wide range of environments, which reported increases in aromaticity following
323 fire (Knicker et al., 2008). Our results also indicate that the changes observed in the DOM and
324 SOM chemistry are unique from one another. It is likely that the changes in aromaticity observed
325 in mineral soils are larger than those reported in the solution-state due to solubility limitations of
326 the aromatic compounds. Therefore, both the mineral soil and water-soluble pools must be
327 evaluated together to identify changes to C and N functionality that impact broader ecosystem
328 functions.

329

330 3.3 Nitrogen composition of 0-5 cm soils was heavily influenced by fire activity

331 To further investigate the influence of fire on soil N species, we focused our analysis on
332 the +ESI spectra, as this method has been reported to increase the compositional coverage of
333 CHNO species compared to -ESI (Roth et al., 2022a). **Table S4** reports the average O, C, N and
334 C:N of each of the 0-5 cm soil samples determined by FT-ICR MS. We found that fire decreased
335 the average C assigned for all burned soils compared to the unburned, though this value was not
336 sensitive to burn severity. Average N per formula was 3x higher than the control for the low and
337 moderate severity soils and was highest for the high severity soil. Increased N content has been
338 reported in laboratory heating studies, attributed Maillard reactions and the formation of covalent
339 bonds between ammonia and organic matter but has not previously been reported from post-fire
340 field studies (Bahureksa et al., 2022; Hestrin et al., 2019). Higher average N in burned soils greatly
341 influenced the C:N ratio of the samples, which was lowest for the low severity soil. Enrichment of
342 N species in burned soils has been observed in controlled lab settings (Bahureksa et al., 2022), and
343 may be attributed to increases in pyridine, benzonitrile, and pyrrole functionalities at higher burn
344 temperatures which were identified in soils affected by the 2013 Rim Fire in California (Chen et
345 al., 2022c). Additionally, lysing of soil microorganisms during soil heating generates labile organic
346 C and N that may contribute to increased dissolved N species following high severity wildfires
347 (Donhauser et al., 2021).

348 Unique N species were compared across the burn severity gradient (Control vs Low, Low
349 vs Moderate, and Moderate vs High) to determine the major changes which occur at each severity
350 (**Table 3**). Because isotopes are not differentiated, there may be additional transformations that are
351 not resolved here. From the control to low burn severity, 9817 unique N species were formed,
352 likely from incomplete combustion of SOM (Bahureksa et al., 2022). Only 297 of the 5632 N
353 species assigned in the control were unique, which indicates that the unique CHNO species in the
354 low severity soil are likely newly formed. There is also a clear change in N speciation through the
355 formation of molecules which are more N-dense (containing more N per molecule), which results
356 in an expanded range of oxygenation and increased N in the low severity soil (**Figure S2A**). From
357 low to moderate severity, 3592 formulas are lost from the low severity soil, and 2153 species are
358 newly formed in the moderate severity sample. Transformations occur across all N classes, and do
359 not appear to preferentially impact any one class over another (**Figure S2B**). From moderate to
360 high severity, the largest losses are in the N₁ class (i.e., compound containing one N atom) and
361 there are substantial increases in the N₃-N₅ class (High) compared to the other transitions. The loss
362 of N₁ formulas was primarily accompanied by a shift towards lower oxygen in the high severity
363 soil from N₁₋₃, and a non-preferential increase in species containing N₄₋₅ (**Figure S2C**). N
364 enrichment may be driven by several combustion-catalyzed processes, including the Maillard
365 reaction pathway and the formation of covalent bonds between burned SOM and NH₃-N

366 (Bahureksa et al., 2022; Hestrin et al., 2019). These results suggest that soils that burned at higher
367 severities contain higher polyaromatic N and are potentially more resistant to microbial
368 degradation. Therefore, the observed decrease in C:N ratios in FT-ICR MS data may indicate a
369 higher proportion of immobilized N, (e.g., as observed in char derived from lignin, cellulose, grass,
370 and wood produced at 350°C and 450°C (Knicker, 2010)) rather than a highly preferential substrate
371 as typically interpreted from C:N alone. Additionally, the N species identified may contribute to
372 increased toxicity in water extracts (Bamba et al., 2017).

373
374 The m/z vs C:N of each CHNO species was plotted in **Figure 3** to visualize differences in
375 molecular mass and N content along the burn severity gradient. We found that although the average
376 mass of the formulas decreased as burn severity increased (**Table S4**), the relative abundance of
377 nitrogenated high molecular weight species increased with burn severity. N-heterocyclic structures
378 are known to form during incomplete combustion of SOM (Knicker et al., 2008), which is thought
379 to be less labile compared to unburned DON. The shift in DON functionality from peptides in
380 unburned soils to polycyclic aromatic compounds (i.e., indoles and carbazoles) (Sharma et al.,
381 2003) likely transforms SOM into a less bioavailable form, of which the microbial genes required
382 for processing may not be widespread in the soil microbiome. To investigate this, we used
383 HMMER (Eddy, 2011) against HMMs curated from UniProt (Bateman et al., 2015) to identify
384 genes that constitute the primary enzyme for degrading carbazole (carbazole 1,9a-dioxigenase)
385 (Nojiri et al., 2005) within the metagenome-assembled genome (MAG) dataset curated from these
386 soils in Nelson et al. (2022) (Nelson et al., 2022). Of the total 637 MAGs, only 13 were actively
387 expressing (via metatranscriptomics data) the majority of the genes required for the
388 multicomponent enzymes (*carAd*, *carAa*, *carAc*), suggesting that these compounds are widely
389 recalcitrant to bacterial degradation. Therefore, newly formed N species may represent an
390 important N sink after fire in high severity burned lodgepole pine soils. Broad shifts in N speciation
391 throughout the burn severity gradient, along with the loss of O-containing functional groups
392 (**Table S4**), may be important for the previously reported differences in soil structure after burn
393 and large alterations in microbial activity (Nelson et al., 2022).

394
395 3.4 The 0-5 cm soils are more influenced by fire than 5-10 cm soils

396 To determine how sampling depth influenced speciation, we compared the control and
397 moderate soils at 0-5 cm and 5-10 cm sampling depths. The 5-10 cm control sample had 17653
398 formulas assigned, 5032 of which contained N. Of the 17870 formulas assigned to the 5-10 cm
399 moderate soil, 6212 were N-containing. The increase in N species for the 5-10 cm soils is much
400 smaller than the 0-5 cm soils, which increased from 5632 in the control to 13813 in the moderate
401 0-5 cm soil. To further investigate the influence of fire on N species in 5-10 cm soils, we plotted
402 the individual heteroatoms (N_xO_x) (**Figure S3**). Between the 0-5 cm and 5-10 cm samples in the
403 control, little variation is noted aside from the 0-5 cm soil being slightly shifted towards lower
404 oxygenation compared to the 5-10 cm soil. There is a clear difference in N content, where the 0-5
405 cm samples are far more N-enriched than the 5-10 cm samples. These results are supported by
406 previous literature indicating that fire generally impacts approximately the top 5 cm of mineral
407 soils, with much less influence of heat further down the soil column (Hartford and Frandsen, 1992).
408 However, we did note some important shifts between the control and moderate 5-10 cm soils, as
409 illustrated in **Figure 4**. Specifically, the moderate severity soil was shifted towards lower oxygen
410 levels, consistent with our observations in the 0-5 cm samples. We also found that the more N-rich
411 species (N_2 - N_4) had far more assignments in the moderate severity soil compared to the control.

412 Therefore, our results indicate that even though the largest effects are seen closer to the soil surface
413 (i.e., 0-5 cm soils), the effects of fire on N speciation persist at least 10 cm down the soil column.
414

415 The relative contribution of all SOM categories determined by solid-state ^{13}C NMR was
416 approximately the same for the 0-5 cm and 5-10 cm samples in the control soil (**Table 1**),
417 consistent with the FT-ICR MS results and indicating that the organic horizon contributed
418 minimally to the overall signal. However, there were notable differences between the 5-10 cm
419 control and moderate severity soils. The relative proportion of *O*-alkyl C decreased by 10, while
420 the aromatic and phenolic C signal increased by 11 in the moderate 5-10 cm soil compared to the
421 control. Differences in the relative proportion of SOM signal indicate that the functional groups
422 present in the soils were affected by the burn, even at the lower sampling depths. The moderate 0-
423 5 cm soil was more aromatic and displayed a lower proportion of *O*-alkyl C than the 5-10 cm
424 sample, consistent with previous studies reporting that the degree of carbonization and
425 aromatization is lower in *Pinus pinaster* mineral soils than in duff (Merino et al., 2018). Because
426 the 5-10 cm soil is not as highly impacted as the 0-5 cm soil, it likely contains more labile substrates
427 for microbial degradation. The alkyl/*O*-alkyl C ratio supports this hypothesis, as the values are
428 lower in the burned 5-10 cm soil than the 0-5 cm soil. Complementary metagenomics analyses
429 indicated major shifts in microbial processing of substrates in 0-5 cm soils, which were not as
430 prevalent in the 5-10 cm soils (Nelson et al., 2022). This suggests that while there are some
431 differences in soil chemistry of the control and moderate 5-10 cm samples, these changes are not
432 nearly as large as those in the 0-5 cm soils.
433

434 3.5 Acute toxicity of soil extract from fire-impacted soils as a function of burn severity

435 Carbon normalized water extracts of six soils were analyzed for acute toxicity by Microtox®
436 to determine toxicity as a function of sample composition. Higher bioluminescence inhibition of
437 *A. fischeri* corresponds to higher acute toxicity. We observed an increase in toxicity with
438 increasing burn severity in the 0-5 cm soils (**Figure 5**), and no change in the 5-10 cm soils. For 0-
439 5 cm soils, the high severity 0-5 cm soil had the highest acute toxicity (43%) followed by moderate
440 severity 0-5 cm soil (17%) and low severity 0-5 cm soil (10%).

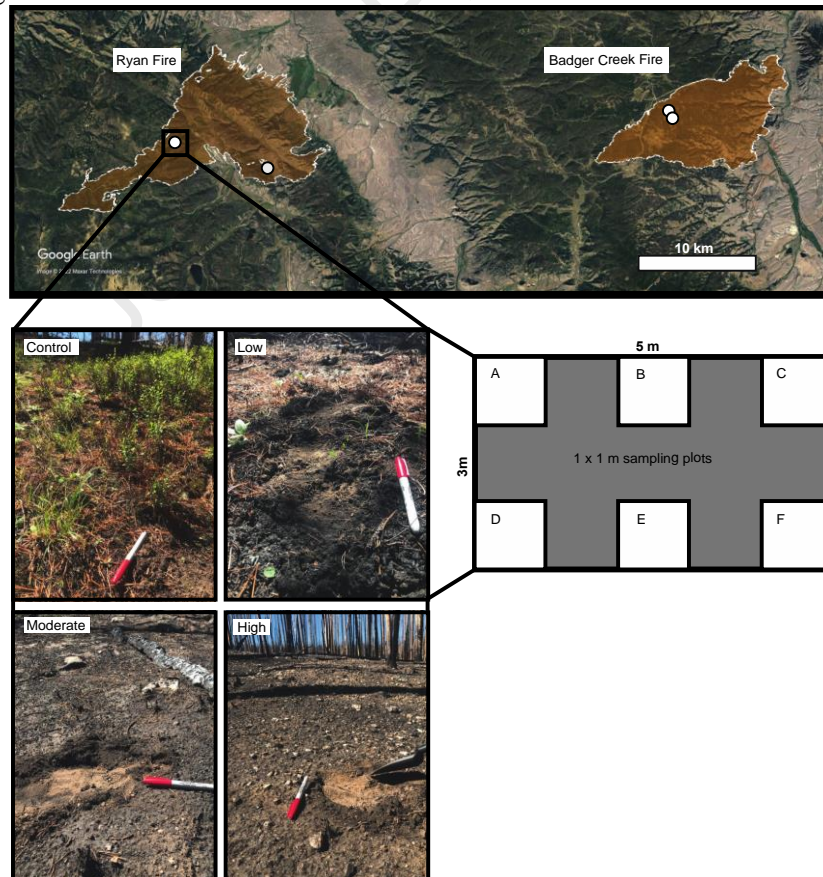
441 Microtox® bioassays have previously been applied to determine the acute toxicity of aqueous
442 ash extracts and runoff following wildfires, both of which inhibited the luminescence of *A. fischeri*
443 (Campos et al., 2012; Silva et al., 2015). Toxicity increases with ash concentration (Silva et al.,
444 2015), and more “complete” combustion in high severity soils may explain the increase in toxicity
445 reported here. A toxicity study using *Daphnia magna* found pH to be a strong influence on toxicity
446 (Harper et al., 2019); however, pH cannot explain the increases in toxicity seen here, as maximum
447 pH values were observed in the moderate severity 0-5 cm soil (average pH = 8.00), whereas the 5-
448 10 cm samples did not appear to be affected (average pH ranging between 7.11 to 7.71) (**Table**
449 **S4**). Previous studies indicated that the formation of N-heterocycles may contribute to increased
450 toxicity (Cervilla et al., 2009), which likely contributes to the observed increase in toxicity here.
451 However, further research is required to identify the specific drivers of toxicity increases in burned
452 organic matter, such as polycyclic aromatic hydrocarbons or heavy metals released during burning.
453 The observed toxicity increase in 0-5 cm soil extracts emphasizes the role of wildfire as a potential
454 source of diffuse contamination for downstream water bodies.
455

476 4 Conclusions

457 Molecular-level analysis of C and N contained in soil organic matter across a burn severity
 458 gradient allowed us to make inferences regarding how organic N is altered by wildfire in high-
 459 elevation forests. Although high-resolution results for a single gradient are reported here, trends
 460 identified from bulk data collected from four burn severity gradients indicate that these results are
 461 likely representative of all the soils we collected. While the analysis of a single gradient does not
 462 allow for statistical analysis, advanced analytical approaches involve rigorous internal calibration
 463 that ensures the resulting data are accurate. Therefore, the molecular-level information provided
 464 by our unique integrative analytical approach provides novel evidence for a potential relationship
 465 between chemistry, toxicity, and the soil microbiome. Our results suggest that N-dense
 466 heterocycles (e.g., carbazoles, indoles) are formed at higher fire severities, which has implications
 467 for post-fire C and N cycling since evidence for processing of these compounds was not
 468 widespread in the local soil microbiome. We noted a shift in N speciation for the 5-10 cm soil
 469 depth, which indicates that heating at that depth was sufficient to shift SOM chemistry. We also
 470 provide evidence that soil toxicity is dependent on burn severity, although further research is
 471 required to identify the specific drivers of soil toxicity and the potential downstream effects.
 472 Collectively, these results emphasize the importance of molecular-level characterization of SOM
 473 components to evaluate the impacts of fire on C and N biogeochemistry and provide new insight
 474 into the impact of severe wildfire on forest ecosystems.

475

476 Tables and Figures



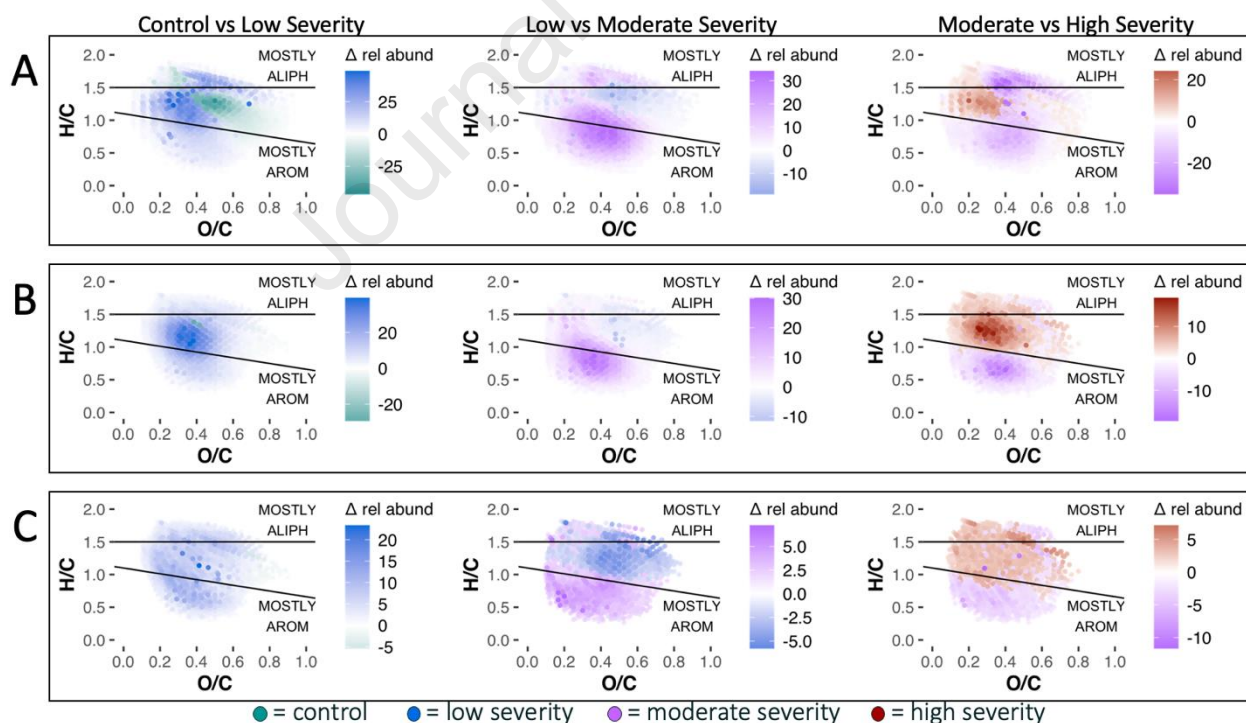
477

478 **Figure 1:** Map indicating sampling sites and strategy in the 2018 Ryan and Badger Creek Fire
 479 burn scars. Top: Google Earth image of the Ryan Fire and Badger Creek Fire burn scars (latitude
 480 of samples ranged from 41.01162 to 41.04866; longitude ranged from -106.12196 to -106.63271).
 481 White dots indicate burn severity transect locations. Bottom left: photos of each burn severity class
 482 (Unburned/Control, Low, Moderate, High Severity). Bottom right: visual representation of the 3x5
 483 m sampling grid with subplots labeled A-F.

484
 485 **Table 1:** Integration results for solid-state ^{13}C NMR spectroscopy analysis of burn severity and
 486 soil depth ($n = 1$). Chemical shift, used to determined NMR regions, is reported in parts per million
 487 (ppm). This table lists the relative proportion of alkyl C, *O*-alkyl C, aromatic & phenolic C, and
 488 carboxylic + carbonyl C to the total signal of ^{13}C across all regions. The alkyl/*O*-alkyl carbon ratio
 489 is determined by dividing the relative proportion of alkyl C by that of the *O*-alkyl C.

Sample	Relative Proportion of SOM categories to the total ^{13}C NMR signal				
	Alkyl C (0-50 ppm)	<i>O</i> -alkyl C (50-100 ppm)	Aromatic & phenolic C (110-165 ppm)	Carboxylic + Carbonyl C (165-210 ppm)	Alkyl/ <i>O</i> -alkyl carbon ratio
Control (0-5 cm)	40	35	20	5	1.14
Low (0-5 cm)	25	11	59	5	2.27
Moderate (0-5 cm)	37	17	39	7	2.18
High (0-5 cm)	35	13	46	6	2.69
Control (5-10 cm)	42	35	19	4	1.20
Moderate (5-10 cm)	41	25	31	3	1.64

490



491 **Figure 2:** van Krevelen diagrams of the detected species of water-soluble soil extracts (0-5 cm)
 492 identified by +ESI FT-ICR MS. The top row (A) contains all formulas, the middle row (B) contains
 493 only CHNO molecular formulas, and the bottom row (C) contains only the unique CHNO species.
 494 Each panel compares two samples, indicated by color. Larger changes in relative abundance (Δ rel
 495

496 abund) are indicated by more saturated colors. Formulas plotted below the line that intercepts at
 497 H/C 1.2 are generally more aromatic in structure, while those plotting above the line that intercepts
 498 at H/C 1.5 are more aliphatic.
 499

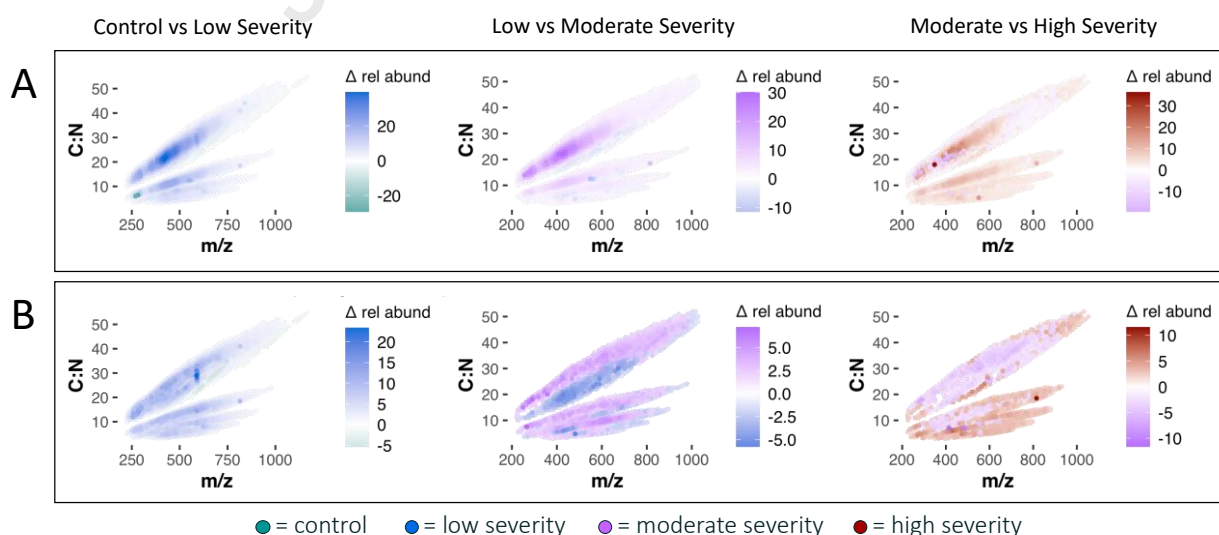
500 **Table 2:** Integration results for solution-state ^1H NMR spectroscopy for the 0-5 cm soil severity
 501 gradient ($n = 1$). Chemical shift is reported in parts per million (ppm). This table lists the relative
 502 proportion of each DOM category to the total signal of ^1H across all regions.

Sample	Relative proportion of soil-derived DOM categories to the total ^1H NMR signal			
	MDLT (0.6-1.6 ppm)	CRAM (1.6-3.2 ppm)	Carbohydrates & peptides (3.2-4.5 ppm)	Aromatic & phenolic (6.5-8.4 ppm)
Control	34	37	22	7
Low	38	31	27	4
Moderate	34	32	25	9
High	36	31	26	7

503
 504 **Table 3:** Unique N species identified through +ESI FT-ICR MS of water-soluble soil extracts (0-
 505 5 cm). Unique formulas are determined only between the two samples compared, denoted in the
 506 top row. N_1 includes molecules containing exactly one N, N_2 includes molecules with two N atoms,
 507 etc.

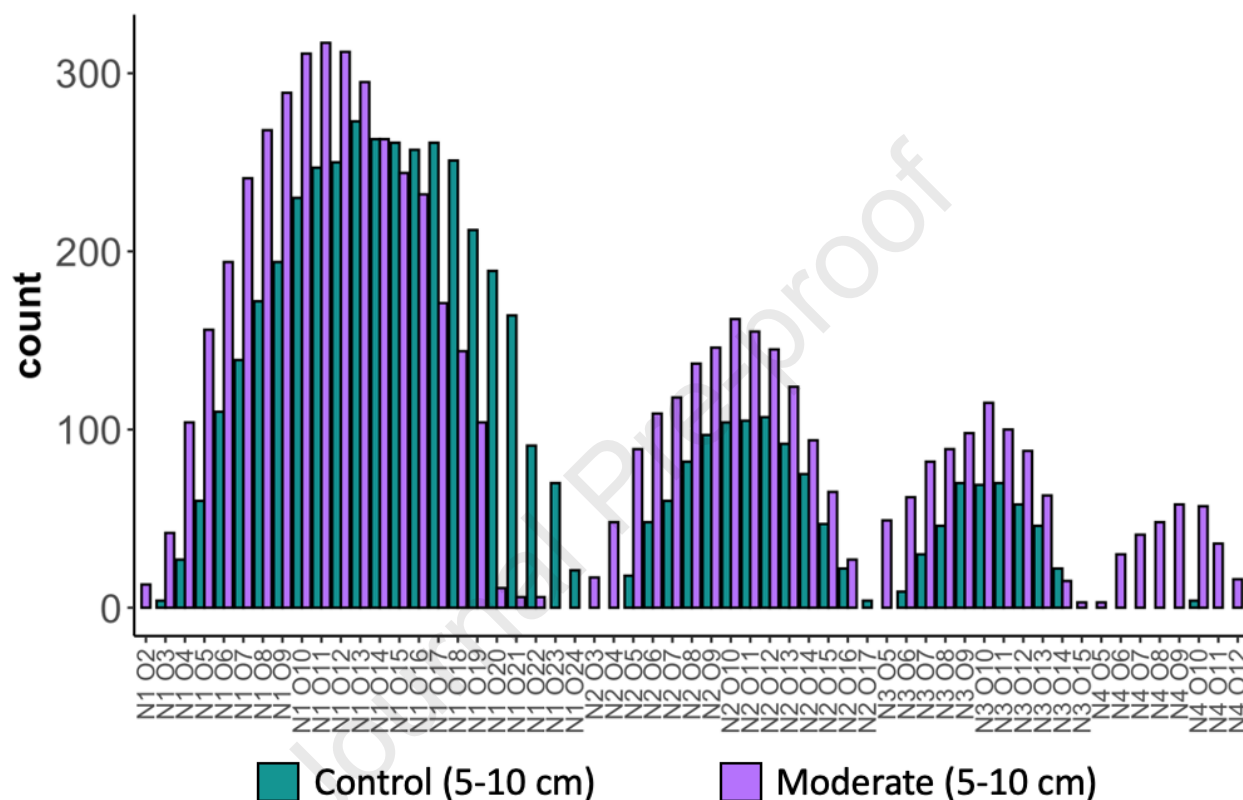
Unique N species	Control vs Low		Low vs Moderate		Moderate vs High	
	Control	Low	Low	Moderate	Moderate	High
All N	297	9817	3592	2153	1499	1932
N_1	295	3464	2091	891	981	358
N_2	2	2850	670	560	346	410
N_3	N/A	1602	378	504	121	532
N_4	N/A	1338	261	126	39	379
N_5	N/A	563	92	72	12	262

508



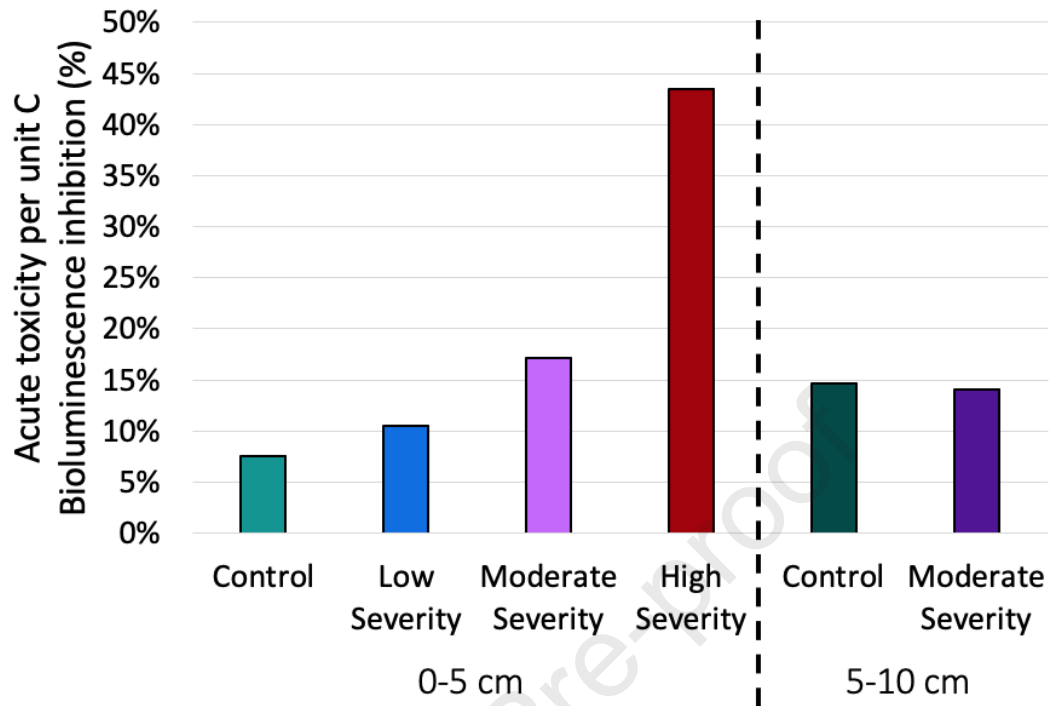
509

510 **Figure 3:** Plots of the mass to charge (m/z) and nitrogen to carbon (N/C) ratios of the N-containing
 511 (i.e., CHNO) fraction obtained via +ESI FT-ICR MS of solid phase extracts of a single Ryan fire
 512 0-5 cm soil burn severity gradient. Panel A displays plots with all the assigned N species; panel B
 513 displays only the unique species between the two spectra. Changes in relative abundance (Δ rel
 514 abund) are indicated by darker colors. Green dots denote higher abundance in the control, and blue,
 515 purple, and red dots correspond to higher abundance in the low, moderate, and high severity
 516 extracts, respectively.
 517



518 **Figure 4:** Nitrogen-containing classes in control and moderate severity 5-10 cm samples ($n = 1$)
 519 from +ESI FT-ICR MS. The x-axis is organized by heteroatoms, grouped first by the number of N
 520 atoms (1-4) assigned to the formulas and second by the number of oxygen atoms. The y-axis
 521 depicts the number of formulas assigned to each heteroatom class.
 522

523



524

525 **Figure 5:** The 15 minute % bioluminescence inhibition of burned soil water extracts (n = 1); higher
526 % inhibition corresponds to higher toxicity.

527

528 Author Information

529 **Corresponding Author: Thomas Borch**

530 Phone: 970-491-6235

531 Email: Thomas.borch@colostate.edu

532

533 Supporting Information

534 Additional experimental details, peak lists, FT-ICR MS spectra and error plots, calculated
535 chemical parameters, FT-ICR MS images can be found in the Supporting Information.

536

537 Acknowledgements

538 DOC and DTN measurements were conducted at the Rocky Mountain Research Station,
539 biogeochemistry laboratory, courtesy of the USDA Forest Service. The authors acknowledge
540 support of MJW and TB from the National Science Foundation under grant number 2114868 and
541 USDA National Institute of Food and Agriculture through AFRI grant number 2021-67019-34608.
542 A portion of the work was performed at the National High Magnetic Field Laboratory ICR User
543 Facility, which is supported by the National Science Foundation Division of Chemistry and
544 Division of Material Research through DMR-1644779 and the State of Florida. M.J.S. thanks the
545 Natural Sciences and Engineering Research Council (NSERC) of Canada for support via a
546 Discovery Grant and the Tier 1 Canada Research Chair in Integrative Molecular Biogeochemistry.

547

548

549

550 References

- 551 Abatzoglou, J.T., Kolden, C.A., Williams, A.P., Lutz, J.A., Smith, A.M.S., 2017. Climatic
552 influences on interannual variability in regional burn severity across western US
553 forests. *Int J Wildland Fire* 26, 269–275. <https://doi.org/10.1071/WF16165>
- 554 Adams, R.H., Domínguez-Rodríguez, V.I., Zavala-Cruz, J., 2015. *Vibrio fischeri* bioassay
555 for determination of toxicity in petroleum contaminated soils from tropical southeast
556 Mexico. *Sains Malays* 44, 337–346.
- 557 Alimoradi, S., Stohr, H., Stagg-Williams, S., Sturm, B., 2020. Effect of temperature on
558 toxicity and biodegradability of dissolved organic nitrogen formed during
559 hydrothermal liquefaction of biomass. *Chemosphere* 238.
560 <https://doi.org/10.1016/j.chemosphere.2019.124573>
- 561 Alizadeh, M.R., Abatzoglou, J.T., Luce, C.H., Adamowski, J.F., Farid, A., Sadegh, M.,
562 2021. Warming enabled upslope advance in western US forest fires. *PNAS* 118.
563 <https://doi.org/10.1073/pnas.2009717118/-/DCSupplemental>
- 564 Andersson, S., Nilsson, S.I., Saetre, P., 2000. Leaching of dissolved organic carbon
565 (DOC) and dissolved organic nitrogen (DON) in mor humus as affected by
566 temperature and pH. *Soil Biology & Biogeochemistry* 32, 1–10.
- 567 Bahureksa, W., Young, R.B., McKenna, A.M., Chen, H., Thorn, K.A., Rosario-Ortiz,
568 F.L., Borch, T., 2022. Nitrogen enrichment during soil organic matter burning and
569 molecular evidence of maillard reactions. *Environ Sci Technol* acs.est.1c06745.
570 <https://doi.org/10.1021/acs.est.1c06745>
- 571 Bamba, D., Coulibaly, M., Robert, D., 2017. Nitrogen-containing organic compounds:
572 Origins, toxicity and conditions of their photocatalytic mineralization over TiO₂.
573 *Science of the Total Environment*. <https://doi.org/10.1016/j.scitotenv.2016.12.130>
- 574 Bateman, A., Martin, M.J., O'Donovan, C., Magrane, M., Apweiler, R., Alpi, E., Antunes,
575 R., Arganiska, J., Bely, B., Bingley, M., Bonilla, C., Britto, R., Bursteinas, B.,
576 Chavali, G., Cibrian-Uhalte, E., da Silva, A., de Giorgi, M., Dogan, T., Fazzini, F.,
577 Gane, P., Castro, L.G., Garmiri, P., Hatton-Ellis, E., Hieta, R., Huntley, R., Legge,
578 D., Liu, W., Luo, J., Macdougall, A., Mutowo, P., Nightingale, A., Orchard, S.,
579 Pichler, K., Poggioli, D., Pundir, S., Pureza, L., Qi, G., Rosanoff, S., Saidi, R.,
580 Sawford, T., Shypitsyna, A., Turner, E., Volynkin, V., Wardell, T., Watkins, X.,
581 Zellner, H., Cowley, A., Figueira, L., Li, W., McWilliam, H., Lopez, R., Xenarios, I.,
582 Bougueleret, L., Bridge, A., Poux, S., Redaschi, N., Aimo, L., Argoud-Puy, G.,
583 Auchincloss, A., Axelsen, K., Bansal, P., Baratin, D., Blatter, M.C., Boeckmann, B.,
584 Bolleman, J., Boutet, E., Breuza, L., Casal-Casas, C., de Castro, E., Coudert, E.,
585 Cuche, B., Doche, M., Dornevil, D., Duvaud, S., Estreicher, A., Famiglietti, L.,
586 Feuermann, M., Gasteiger, E., Gehant, S., Gerritsen, V., Gos, A., Gruaz-Gumowski,
587 N., Hinz, U., Hulo, C., Jungo, F., Keller, G., Lara, V., Lemercier, P., Lieberherr, D.,
588 Lombardot, T., Martin, X., Masson, P., Morgat, A., Neto, T., Nospikel, N., Paesano,
589 S., Pedruzzi, I., Pilbout, S., Pozzato, M., Pruess, M., Rivoire, C., Roechert, B.,
590 Schneider, M., Sigrist, C., Sonesson, K., Staehli, S., Stutz, A., Sundaram, S.,
591 Tognolli, M., Verbregue, L., Veuthey, A.L., Wu, C.H., Arighi, C.N., Arminski, L.,
592 Chen, C., Chen, Y., Garavelli, J.S., Huang, H., Laiho, K., McGarvey, P., Natale,
593 D.A., Suzek, B.E., Vinayaka, C.R., Wang, Q., Wang, Y., Yeh, L.S., Yerramalla,
594 M.S., Zhang, J., 2015. UniProt: A hub for protein information. *Nucleic Acids Res* 43,
595 D204–D212. <https://doi.org/10.1093/nar/gku989>

- 596 Belov, M.E., Rakov, V.S., Nikolaev, E.N., Goshe, M.B., Anderson, G.A., Smith, R.D.,
597 2003. Initial implementation of external accumulation liquid
598 chromatography/electrospray ionization fourier transform ion cyclotron resonance
599 with automated gain control. *Rapid Communications in Mass Spectrometry* 17, 627–
600 636. <https://doi.org/10.1002/rcm.955>
- 601 Bodí, M.B., Martin, D.A., Balfour, V.N., Santín, C., Doerr, S.H., Pereira, P., Cerdà, A.,
602 Mataix-Solera, J., 2014. Wildland fire ash: Production, composition and eco-hydro-
603 geomorphic effects. *Earth Sci Rev* 130, 103–127.
604 <https://doi.org/10.1016/j.earscirev.2013.12.007>
- 605 Caiafa, M. V., Nelson, A.R., Borch, T., Roth, H.K., Fegel, T.S., Rhoades, C.C., Wilkins,
606 M.J., Glassman, S.I., 2023. Distinct fungal and bacterial responses to fire severity
607 and soil depth across a ten-year wildfire chronosequence in beetle-killed lodgepole
608 pine forests. SSRN. <https://doi.org/10.2139/ssrn.4372834>
- 609 Campos, I., Abrantes, N., Vidal, T., Bastos, A.C., Gonçalves, F., Keizer, J.J., 2012.
610 Assessment of the toxicity of ash-loaded runoff from a recently burnt eucalypt
611 plantation. *Eur J For Res* 131, 1889–1903. [https://doi.org/10.1007/s10342-012-0640-](https://doi.org/10.1007/s10342-012-0640-7)
612 [7](https://doi.org/10.1007/s10342-012-0640-7)
- 613 Cervilla, L.M., Blasco, B., Ríos, J.J., Rosales, M.A., Rubio-Wilhelmi, M.M., Sánchez-
614 Rodríguez, E., Romero, L., Ruiz, J.M., 2009. Response of nitrogen metabolism to
615 boron toxicity in tomato plants. *Plant Biol (Stuttg)* 11, 671–677.
616 <https://doi.org/10.1111/j.1438-8677.2008.00167.x>
- 617 Chen, H., Ersan, M.S., Tolić, N., Chu, R.K., Karanfil, T., Chow, A.T., 2022a. Chemical
618 characterization of dissolved organic matter as disinfection byproduct precursors by
619 UV/fluorescence and ESI FT-ICR MS after smoldering combustion of leaf needles
620 and woody trunks of pine (*Pinus jeffreyi*). *Water Res* 209.
621 <https://doi.org/10.1016/j.watres.2021.117962>
- 622 Chen, H., McKenna, A.M., Niles, S.F., Frye, J.W., Glatke, T.J., Rodgers, R.P., 2022b.
623 Time-dependent molecular progression and acute toxicity of oil-soluble,
624 interfacially-active, and water-soluble species reveals their rapid formation in the
625 photodegradation of Macondo Well Oil. *Science of the Total Environment* 813.
626 <https://doi.org/10.1016/j.scitotenv.2021.151884>
- 627 Chen, H., Wang, J.-J., Ku, P.-J., Tsui, M.T.-K., Abney, R.B., Berhe, A.A., Zhang, Q.,
628 Burton, S.D., Dahlgren, R.A., Chow, A.T., 2022c. Burn intensity drives the alteration
629 of phenolic lignin to (Poly) aromatic hydrocarbons as revealed by pyrolysis gas
630 chromatography–mass spectrometry (Py-GC/MS). *Environ Sci Technol*.
631 <https://doi.org/10.1021/acs.est.2c00426>
- 632 Corilo, Y.E., 2014. PetroOrg Software.
- 633 D’Andrilli, J., Cooper, W.T., Foreman, C.M., Marshall, A.G., 2015. An ultrahigh-
634 resolution mass spectrometry index to estimate natural organic matter lability. *Rapid*
635 *Communications in Mass Spectrometry* 29, 2385–2401.
636 <https://doi.org/10.1002/rcm.7400>
- 637 Dittmar, T., Koch, B., Hertkorn, N., Kattner, G., 2008. A simple and efficient method for
638 the solid-phase extraction of dissolved organic matter (SPE-DOM) from seawater.
639 *Limnol Oceanogr Methods* 6, 230–235.
- 640 Doherty, F.G., 2001. A Review of the Microtox ® toxicity test system for assessing the
641 toxicity of sediments and soils. *Water Qual. Res. J. Canada* 36, 475–518.

- 642 Donhauser, J., Qi, W., Bergk-Pinto, B., Frey, B., 2021. High temperatures enhance the
643 microbial genetic potential to recycle C and N from necromass in high-mountain
644 soils. *Glob Chang Biol* 27, 1365–1386. <https://doi.org/10.1111/gcb.15492>
- 645 Dzwonko, Z., Loster, S., Gawroński, S., 2015. Impact of fire severity on soil properties
646 and the development of tree and shrub species in a Scots pine moist forest site in
647 southern Poland. *For Ecol Manage* 342, 56–63.
648 <https://doi.org/10.1016/j.foreco.2015.01.013>
- 649 Eddy, S.R., 2011. Accelerated profile HMM searches. *PLoS Comput Biol* 7.
650 <https://doi.org/10.1371/journal.pcbi.1002195>
- 651 Emmett, M.R., White, F.M., Hendrickson, C.L., Shi, D.H., Marshall, A.G., 1998.
652 Application of micro-electrospray liquid chromatography techniques to FT-ICR MS
653 to enable high-sensitivity biological analysis. *J Am Soc Mass Spectrom* 9, 333–340.
654 [https://doi.org/10.1016/S1044-0305\(97\)00287-0](https://doi.org/10.1016/S1044-0305(97)00287-0)
- 655 Gavrić, S., Flanagan, K., Österlund, H., Blecken, G.T., Viklander, M., 2022. Facilitating
656 maintenance of stormwater ponds: comparison of analytical methods for
657 determination of metal pollution. *Environmental Science and Pollution Research* 29,
658 74877–74893. <https://doi.org/10.1007/s11356-022-20694-0>
- 659 González-Pérez, J.A., González-Vila, F.J., Almendros, G., Knicker, H., 2004. The effect
660 of fire on soil organic matter - A review. *Environ Int* 30, 855–870.
661 <https://doi.org/10.1016/j.envint.2004.02.003>
- 662 Harper, A.R., Santin, C., Doerr, S.H., Froyd, C.A., Albin, D., Otero, X.L., Viñas, L.,
663 Pérez-Fernández, B., 2019. Chemical composition of wildfire ash produced in
664 contrasting ecosystems and its toxicity to *Daphnia magna*. *Int J Wildland Fire* 28,
665 726–737. <https://doi.org/10.1071/WF18200>
- 666 Hartford, R.A., Frandsen, W.H., 1992. When it's hot, it's hot ... or maybe it's not!
667 (Surface flaming may not portend extensive soil heating), *Int. J. Wildland Fire*.
- 668 Hendrickson, C.L., Quinn, J.P., Kaiser, N.K., Smith, D.F., Blakney, G.T., Chen, T.,
669 Marshall, A.G., Weisbrod, C.R., Beu, S.C., 2015. 21 Tesla fourier transform ion
670 cyclotron resonance mass spectrometer: A national resource for ultrahigh resolution
671 mass analysis. *J Am Soc Mass Spectrom* 26, 1626–1632.
672 <https://doi.org/10.1007/s13361-015-1182-2>
- 673 Hestrin, R., Torres-Rojas, D., Dynes, J.J., Hook, J.M., Regier, T.Z., Gillespie, A.W.,
674 Smernik, R.J., Lehmann, J., 2019. Fire-derived organic matter retains ammonia
675 through covalent bond formation. *Nat Commun* 10, 1–8.
676 <https://doi.org/10.1038/s41467-019-08401-z>
- 677 Key, C.H., Benson, N.C., 2006. Landscape assessment (LA) sampling and analysis
678 methods. USDA Forest Service Gen Tech. Rep RMRS-GTR-164-CD.
- 679 Kim, S., Kramer, R.W., Hatcher, P.G., 2003. Graphical method for analysis of ultrahigh-
680 resolution broadband mass spectra of natural organic matter, the Van Krevelen
681 diagram. *Anal Chem* 75, 5336–5344. <https://doi.org/10.1021/ac034415p>
- 682 Knicker, H., 2010. “Black nitrogen” - an important fraction in determining the
683 recalcitrance of charcoal. *Org Geochem* 41, 947–950.
684 <https://doi.org/10.1016/j.orggeochem.2010.04.007>
- 685 Knicker, H., Hilscher, A., González-Vila, F.J., Almendros, G., 2008. A new conceptual
686 model for the structural properties of char produced during vegetation fires. *Org*
687 *Geochem* 39, 935–939. <https://doi.org/10.1016/j.orggeochem.2008.03.021>

- 688 Luo, L., Chen, Z., Lv, J., Cheng, Y., Wu, T., Huang, R., 2019. Molecular understanding of
689 dissolved black carbon sorption in soil-water environment. *Water Res* 154, 210–216.
690 <https://doi.org/10.1016/j.watres.2019.01.060>
- 691 Merino, A., Chávez-Vergara, B., Salgado, J., Fonturbel, M.T., García-Oliva, F., Vega,
692 J.A., 2015. Variability in the composition of charred litter generated by wildfire in
693 different ecosystems. *Catena (Amst)* 133, 52–63.
694 <https://doi.org/10.1016/j.catena.2015.04.016>
- 695 Merino, A., Fonturbel, M.T., Fernández, C., Chávez-Vergara, B., García-Oliva, F., Vega,
696 J.A., 2018. Inferring changes in soil organic matter in post-wildfire soil burn severity
697 levels in a temperate climate. *Science of the Total Environment* 627, 622–632.
698 <https://doi.org/10.1016/j.scitotenv.2018.01.189>
- 699 Moody, J.A., Shakesby, R.A., Robichaud, P.R., Cannon, S.H., Martin, D.A., 2013.
700 Current research issues related to post-wildfire runoff and erosion processes. *Earth*
701 *Sci Rev* 122, 10–37. <https://doi.org/10.1016/j.earscirev.2013.03.004>
- 702 Nave, L.E., Vance, E.D., Swanston, C.W., Curtis, P.S., 2011. Fire effects on temperate
703 forest soil C and N storage. *Ecological Applications* 21, 1189–1201.
704 <https://doi.org/10.1890/10-0660.1>
- 705 Nelson, A.R., Narrowe, A.B., Rhoades, C.C., Fegél, T.S., Daly, R.A., Roth, H.K., Chu,
706 R.K., Amundson, K.K., Young, R.B., Steindorff, A.S., Mondo, S.J., Grigoriev, I. V.,
707 Salamov, A., Borch, T., Wilkins, M.J., 2022. Wildfire-dependent changes in soil
708 microbiome diversity and function. *Nat Microbiol.* [https://doi.org/10.1038/s41564-](https://doi.org/10.1038/s41564-022-01203-y)
709 [022-01203-y](https://doi.org/10.1038/s41564-022-01203-y)
- 710 Nojiri, H., Ashikawa, Y., Noguchi, H., Nam, J.W., Urata, M., Fujimoto, Z., Uchimura, H.,
711 Terada, T., Nakamura, S., Shimizu, K., Yoshida, T., Habe, H., Omori, T., 2005.
712 Structure of the terminal oxygenase component of angular dioxygenase, carbazole
713 1,9a-dioxygenase. *J Mol Biol* 351, 355–370.
714 <https://doi.org/10.1016/j.jmb.2005.05.059>
- 715 Page, J.S., Bogdanov, B., Vilkov, A.N., Prior, D.C., Buschbach, M.A., Tang, K., Smith,
716 R.D., 2005. Automatic gain control in mass spectrometry using a jet disrupter
717 electrode in an electrodynamic ion funnel. *J Am Soc Mass Spectrom* 16, 244–253.
718 <https://doi.org/10.1016/j.jasms.2004.11.003>
- 719 Parsons, A., Robichaud, P.R., Lewis, S.A., Napper, C., Clark, J.T., 2010. Field Guide for
720 Mapping Post-Fire Soil Burn Severity. General Technical Report RMRS-GTR-243 .
- 721 Pulido-Chavez, M.F., Alvarado, E.C., DeLuca, T.H., Edmonds, R.L., Glassman, S.I.,
722 2021. High-severity wildfire reduces richness and alters composition of
723 ectomycorrhizal fungi in low-severity adapted ponderosa pine forests. *For Ecol*
724 *Manage* 485. <https://doi.org/10.1016/j.foreco.2021.118923>
- 725 Rhoades, C.C., Chow, A.T., Covino, T.P., Fegél, T.S., Pierson, D.N., Rhea, A.E., 2018.
726 The legacy of a severe wildfire on stream nitrogen and carbon in headwater
727 catchments. *Ecosystems.* <https://doi.org/10.1007/s10021-018-0293-6>
- 728 Roth, H.K., Borch, T., Young, R.B., Bahureksa, W., Blakney, G.T., Nelson, A.R.,
729 Wilkins, M.J., McKenna, A.M., 2022a. Enhanced speciation of pyrogenic organic
730 matter from wildfires enabled by 21 T FT-ICR mass spectrometry. *Anal Chem*
731 *acs.analchem.1c05018.* <https://doi.org/10.1021/acs.analchem.1c05018>
- 732 Roth, H.K., Nelson, A.R., McKenna, A.M., Fegél, T.S., Young, R.B., Rhoades, C.C.,
733 Wilkins, M.J., Borch, T., 2022b. Impact of beaver ponds on biogeochemistry of

- 734 organic carbon and nitrogen along a fire-impacted stream. *Environ Sci Process*
735 *Impacts* 24, 1661–1677. <https://doi.org/10.1039/D2EM00184E>
- 736 Schmidt, M.W.I., Noack, A.G., 2000. Black carbon in soils and sediments: Analysis,
737 distribution, implications, and current challenges. *Global Biogeochem Cycles*.
738 <https://doi.org/10.1029/1999GB001208>
- 739 Schmidt, M.W.I., Torn, M.S., Abiven, S., Dittmar, T., Guggenberger, G., Janssens, I.A.,
740 Kleber, M., Kögel-Knabner, I., Lehmann, J., Manning, D.A.C., Nannipieri, P., Rasse,
741 D.P., Weiner, S., Trumbore, S.E., 2011. Persistence of soil organic matter as an
742 ecosystem property. *Nature* 478, 49–56. <https://doi.org/10.1038/nature10386>
- 743 Sharma, R.K., Chan, W.G., Seeman, J.I., Hajaligol, M.R., 2003. Formation of low
744 molecular weight heterocycles and polycyclic aromatic compounds (PACs) in the
745 pyrolysis of α -amino acids. *J. Anal. Appl. Pyrolysis* 66, 97–121.
- 746 Silva, V., Pereira, J.L., Campos, I., Keizer, J.J., Gonçalves, F., Abrantes, N., 2015.
747 Toxicity assessment of aqueous extracts of ash from forest fires. *Catena (Amst)* 135,
748 401–408. <https://doi.org/10.1016/j.catena.2014.06.021>
- 749 Simpson, M.J., Otto, A., Feng, X., 2008. Comparison of Solid-State Carbon-13 Nuclear
750 magnetic resonance and organic matter biomarkers for assessing soil organic matter
751 degradation. *Soil Science Society of America Journal* 72, 268–276.
752 <https://doi.org/10.2136/sssaj2007.0045>
- 753 Singh, N., Abiven, S., Torn, M.S., Schmidt, M.W.I., 2012. Fire-derived organic carbon in
754 soil turns over on a centennial scale. *Biogeosciences* 9, 2847–2857.
755 <https://doi.org/10.5194/bg-9-2847-2012>
- 756 Smith, D.F., Podgorski, D.C., Rodgers, R.P., Blakney, G.T., Hendrickson, C.L., 2018. 21
757 Tesla FT-ICR mass spectrometer for ultrahigh-resolution analysis of complex
758 organic mixtures. *Anal Chem* 90, 2041–2047.
759 <https://doi.org/10.1021/acs.analchem.7b04159>
- 760 Smolander, Aino, Kitunen, Veikko, Mälkönen, Eino, Smolander, A, Kitunen, V,
761 Mälkönen, E, 2001. Dissolved soil organic nitrogen and carbon in a Norway spruce
762 stand and an adjacent clear-cut, *Biol Fertil Soils*. Springer-Verlag.
- 763 Turner, M.G., 2010. Disturbance and landscape dynamics in a changing world 91, 2833–
764 2849.
- 765 Wan, S., Hui, D., Luo, Y., 2001. FIRE EFFECTS ON NITROGEN POOLS AND
766 DYNAMICS IN TERRESTRIAL ECOSYSTEMS: A META-ANALYSIS,
767 Ecological Applications.
- 768 Westerling, A.L.R., 2016. Increasing western US forest wildfire activity: Sensitivity to
769 changes in the timing of spring. *Philosophical Transactions of the Royal Society B:*
770 *Biological Sciences* 371. <https://doi.org/10.1098/rstb.2015.0178>
- 771 Williams, A.P., Abatzoglou, J.T., 2016. Recent Advances and Remaining Uncertainties in
772 Resolving Past and Future Climate Effects on Global Fire Activity. *Curr Clim*
773 *Change Rep*. <https://doi.org/10.1007/s40641-016-0031-0>
- 774 Xu, P., Yu, B., Li, F.L., Cai, X.F., Ma, C.Q., 2006. Microbial degradation of sulfur,
775 nitrogen and oxygen heterocycles. *Trends Microbiol*.
776 <https://doi.org/10.1016/j.tim.2006.07.002>
- 777 Zhong, Z., Makeschin, F., 2003. Soluble organic nitrogen in temperate forest soils. *Soil*
778 *Biology & Biogeochemistry* 35, 333–338.
- 779

- Higher burn severities result in the formation of N-dense molecules
- The soil microbiome is largely unable to process N-dense molecules
- Soil toxicity increases as burn severity increases

Journal Pre-proof

Declaration of interests

The authors declare that they have no known competing financial interests or personal relationships that could have appeared to influence the work reported in this paper.

The authors declare the following financial interests/personal relationships which may be considered as potential competing interests:

Thomas Borch reports financial support was provided by National Science Foundation. Thomas Borch reports financial support was provided by USDA National Institute of Food and Agriculture through AFRI.